REENTRANT WAVES INDUCED BY LOCAL BISTABILITIES IN A CARDIAC MODEL

S. Bahar
Box 90305, Department of Physics, Duke University, Durham NC 27708, USA
bahar@phy.duke.edu

Abstract

Rate-dependent bistability and hysteresis have recently been observed to be highly prevalent in periodically stimulated bullfrog ventricular muscle. Similar bistabilities have been found in *in vivo* sheep atria at interstimulus intervals for which spatiotemporally complex behaviors, possibly atrial flutter and fibrillation, are observed. Might bistability play a role in the onset of spatiotemporal disorganization in the whole heart? We investigate the role of local bistability in a coupled map/cellular automaton model of cardiac dynamics. This two-dimensional model is based on a simple mapping which gives good qualitative agreement with many of the local features of cardiac dynamics. Under some conditions, local regions of bistability are found to result in phase singularities and rotors in the spatially extended model presented here.

Introduction and Background

Different patterns of dynamical response can be elicited under different conditions in cardiac tissue. For example, when stimuli are delivered at a slow rate, one action potential response is elicited for every stimulus (denoted as a 1:1 state). As the stimulus rate (basic cycle length, or BCL) is increased, the action potential duration (APD) begins to oscillate, entering a state called "alternans", in which every stimulus elicits a response but the responses are of alternating duration (2:2 state) [1,2,3]. As the stimulus rate is increased further, the tissue becomes unable to recover fast enough to respond to every applied stimulus, resulting in a pattern of "skipped beats", where every other stimulus elicits a response (2:1 pattern). Under other conditions (e.g., different range of applied current amplitude), more complicated behaviors arise [4,5,6].

As pointed out by Guevara *et al.* [2], rate-dependent bistability and hysteresis between 1:1 (or 2:2) and 2:1 states can occur in simple models of cardiac dynamics as the interstimulus interval (here called BCL, or basic cycle length) is swept up and down. Bistability between the 1:1 branch and the 2:1 branch of APD response was first observed experimentally by Mines in 1913 in a bullfrog cardiac preparation [7], and later by Guevara *et al.* [4] in an aggregate of spontaneously beating chick embryonic ventricular myocytes. Recently it has been shown that bistability is a highly prevalent local behavior in bullfrog ventricular myocardium, occurring in 74% of preparations studied [8]. Bistability was subsequently observed in *in vivo* sheep atrium for BCL values over which arrhythmias and spatiotemporal disorganization (possibly flutter or fibrillation) also occurred [9]. **Can local bistabilities play a role in the onset of spatial disorganization in excitable media?** We investigate this question using a simple cardiac model.

The Model

Experimentally it has been found [3] that APD_n is dependent on the previous diastolic interval DI_{n-1}, i.e.,

$$APD_{n-}=f(DI_{n-1}) \quad (1)$$

where the diastolic interval is defined as

$$DI_{n-1}=N*BCL-APD_{n-1}. \quad (2)$$

Here, N is the smallest integer such that

$$N*BCL>APD_{n-1}+\theta \quad (3)$$

where θ is the minimal diastolic interval the tissue can sustain. The experimentally measured values of APD_n and DI_{n-1} can be fit with an exponential function

$$APD_n=A_o-Ae^{-DI_{n-1}/\tau} \quad (4)$$

which, after substituting (1), constitutes a mapping which takes APD_{n-1} into APD_n [2,3]. When the slope of the function f is of magnitude less than one, there is a single steady state solution, corresponding to the 1:1 state. When the magnitude of the slope of f exceeds unity, the 1:1 solution becomes unstable and a stable 2:2 solution is born through a forward bifurcation [10]. When $BCL-APD_n$ falls below θ, the tissue can only recover fast enough to respond to every other stimulus, and the system moves to the 2:1 branch (N=2). While only a simple approximation to cardiac dynamics, this model does preserve many of the observed features of experimental preparations (transitions from 1:1 to 2:2, bistability between N=1 and N=2 branches).

The coupled map/cellular automaton model considered here consists of a 170 by 170 grid of elements, with a map of the form (2)-(4) at each element, with parameters A_o=290 msec, A=203 msec, τ=187 msec and θ=-20 msec. The window of bistability occurs for BCL values 118 msec to 185 msec. (Compare the physically observed range of BCL values, 90 msec to 160 msec, over which bistability is observed *in vivo* in sheep atrium [9].) Each element in the grid can exist in one of three states, defined as follows:

State 0. *In this "off" or "excitable" state, the element is considered to have recovered from its previous action potential and to be susceptible to stimulation by its neighbors. In this state the element cannot excite its neighbors.*

State 1. *An "on", state, where the element is considered capable of exciting its neighbors, but is not susceptible to stimulation by neighboring elements.*

State 2. *A "refractory" state, where the element cannot excite its neighbors or be excited by them.*

The dwell time of each element in a particular state is determined by the states of the neighboring elements and by the mapping model. We define a variable APD_{ij}^t at each element, where i and j are the element's coordinates in the grid, and t is the number of total timesteps in the simulation (each update of the map is a timestep of 1 msec). We define the phase P_{ij}^t as the time since the last activation at coordinates (i,j). At each update of the lattice, P_{ij}^t at coordinates where an activation does not occur is advanced by 1 msec, and the APD_{ij}^t is unchanged. When the element (i,j) is excited by a neighbor, P_{ij}^t is reset to 1 and APD_{ij}^t is calculated using the previous APD_{ij}^t according to the map (2)-(4), **with BCL=P_{ij}^t**. The state of an element at time t is determined from P_{ij}^t and APD_{ij}^t as follows:

$$P_{ij}^{t-1} < \sigma_1 (APD_{ij}^{t} + \theta) \rightarrow \text{state1}$$
$$\sigma_1 (APD_{ij}^{t} + \theta) \leq P_{ij}^{t-1} \leq (APD_{ij}^{t} + \theta) \rightarrow \text{state2}$$
$$P_{ij}^{t-1} > (APD_{ij}^{t} + \theta) \rightarrow \text{state0}$$

Thus during some early fraction σ_1 of the action potential duration the element is in its excited state (state 1). After this period the element enters a refractory state (state 2), which lasts $(1-\sigma_1)(APD_{ij}^{t}+\theta)$ msec. After a total time $(APD_{ij}^{t}+\theta)$ msec since its activation, the element returns to an excitable state (state 0).

Coupling between the elements of the map is defined as follows: in each timestep t an element (i,j) can be excited by its three nearest neighbors in the longitudinal directions, its two nearest neighbors in the transverse directions, and its closest nearest neighbors diagonally. This results in "propagation" consistent with the distribution of conduction velocities in ventricular myocardium, where excitation propagates three times as fast along the longitudinal direction as along the transverse direction [11]. Each element is be considered to approximate a group of 3 X 3 cells, and the entire array an 51 mm by 10 mm piece of "tissue". In the simulations illustrated here we have stretched the aspect ratio in order to elongate the vertical direction.

Simple Periodic Stimulation

To simulate periodic stimulation of the "tissue", we deliver a stimulus to one element of the grid at intervals BCL. In Figure 1, we show a sequence of snapshots of the coupled map model as it is periodically stimulated with a BCL of 150 msec.

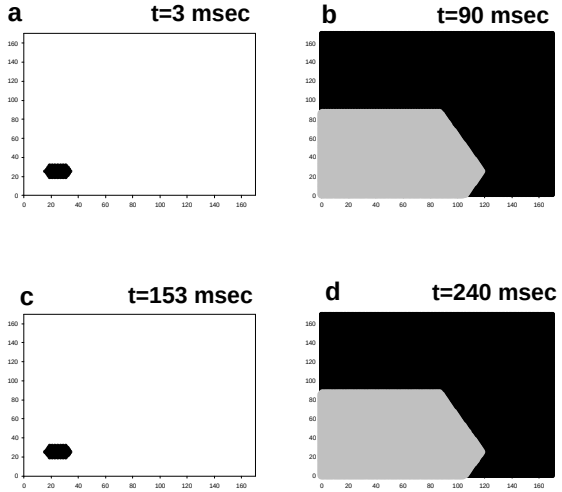

Fig. 1 Snapshots of a simulation with σ_1=0.60. All elements (i,j) are initially set with APD_{ij}^{0}=118.5 msec, the steady state value on the N=1 branch at BCL=150 msec. Periodic stimulation at BCL=150 msec is delivered from element (25,25). In Frame 1a, a small region of elements centered about (25,25) has become excited (state 1, black region), while the rest of the tissue is unexcited (state 0, white region). In frame 1b, at t=90 msec, the excited region has spread to the boundaries of the "tissue", and the center region is now in a refractory state (state 2, grey region). When another stimulus is delivered at t=150 msec, the tissue is ready to respond (frames c and d).

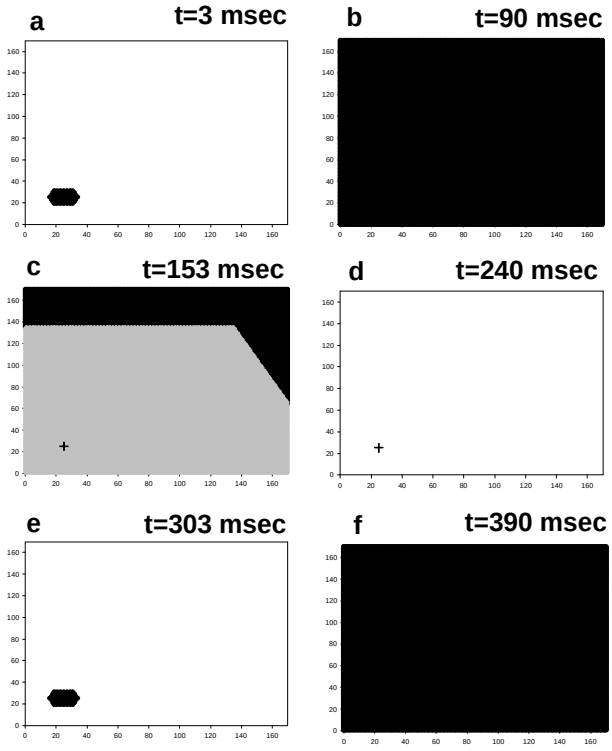

Fig. 2 Snapshots from a simulation with conditions identical to Fig. 1, except that the initial conditions APD_{ij}^{0} are set to 182 msec, the steady state value of APD on the N=2 branch at BCL=150 msec. Since APD+θ >BCL, the tissue at the pacing site (25,25) is still refractory at t=150 msec, as shown in Fig 2c. No response is elicited by a stimulus delivered at this point (marked with an x). By t=240, the tissue has recovered, shown in Fig. 2d. At t=2BCL=300 msec, the tissue is ready to respond again to an applied stimulus. This illustrates a 2:1 pattern, in contrast to the 1:1 pattern shown in Fig 1.

In Figure 2 we show results from a run identical to that shown in Fig. 1, except that APD_{ij}^{0}=182 msec. Here, the first stimulus propagates as before (2a, b). However, the second stimulus elicits no response (c), since the APD on the 2:1 branch gives APD+θ >BCL, and thus the element (25,25) is still in a refractory state (state 2) when the second stimulus is given. By the time the third stimulus is delivered, however, the tissue has returned to its excitable state (state 0), and is now ready to respond, as shown in (e,f). The patterns shown in Figs. 1 and 2 are bistable -- they coexist for the same set of parameter values, and the system falls into one pattern or another depending on initial conditions.

Reentrant Waves, Phase Singularities and Rotors: A Small Region of 2:1

Suppose that a small region of the map, though in phase with its neighbors, has fallen onto the initial conditions for another branch. Specifically, suppose we have the entire tissue initially in a 1:1 state, except for a small region in a 2:1 state. In order for the 2:1 region to remain active until the surrounding 1:1 wavefront has passed, we must require

$$\sigma_1(APD_2+\theta) > APD_1+\theta.$$

If this condition is met, the active 2:1 elements will “reenter” the recovered region in the wake of the passing front, and restimulate the just-recovered 1:1 elements.

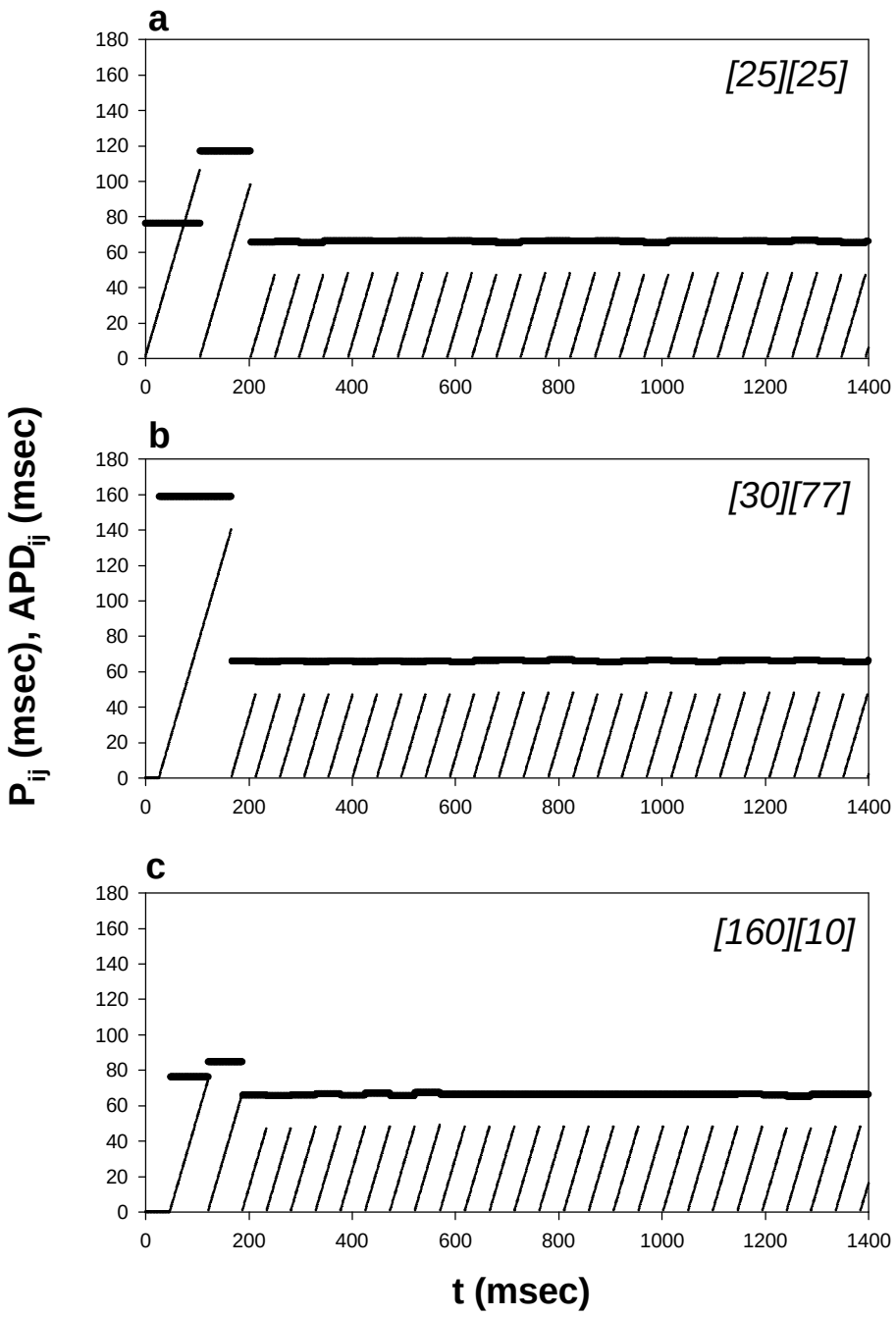

Fig. 3. Phase resetting plots for a simulation in which the "1:1" elements are set with APD_{ij}^{0}=78.85 msec, a value in the basin of attraction of the 1:1 fixed point (APD=103.82 msec) at BCL=120 msec. A strip of elements (j=75 to 78, i=20 to 80) is set with APD_{ij}^{0}=158.63 msec, the 2:1 fixed point at this BCL. Periodic stimulation is delivered from element [25][25] at BCL=120 msec. Panels show the evolution of P_{ij}^{t} and APD_{ij}^{t} at (a) the stimulation site, (b) an element in the reentrant 2:1 region and (c) and an element initially on the "1:1" (or "transient 2:2") branch. By t=200 msec, all elements are being periodically stimulated by the rotor at intervals T_f. Coordinates [i][j] are shown in the top right corner of each panel.

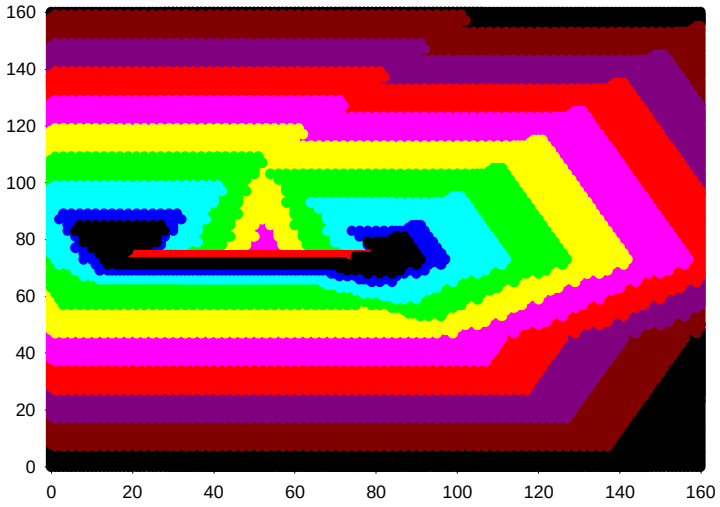

Fig. 4 A phase singularity in the simulation illustrated in Fig. 3, at t=235 msec. Because of the size and location of the strip of 2:1 elements with respect to the stimulation site, reexcitation of the recovered tissue by the 2:1 elements generates a clearly visible pair of "twin rotors". The locations of the rotor cores do not appear to drift during the duration of the simulation. Color code: black: $0<P_{ij}\leq 10$, brown: $10<P_{ij}\leq 15$, purple: $15<P_{ij}\leq 20$, orange: $20<P_{ij}\leq 25$, magenta: $25<P_{ij}\leq 30$, yellow: $30<P_{ij}\leq 35$, green: $35<P_{ij}\leq 40$, light blue: $40<P_{ij}\leq 45$,dark blue: $P_{ij}> 45$.

Once this "reentry" has occurred, what happens next? The crucial thing is that the restimulation of the recovered 1:1 elements creates a phase singularity (Figure 4). If the 1:1 elements are all placed squarely on the 1:1 fixed point, the singularity is drowned out by the periodic stimuli delivered from the pacing site. However, we find that if the 1:1 elements are in a state of transiently alternating about the 1:1 steady state (i.e., in the basin of attraction but not at the fixed point), then the singularity acts as a self-sustaining rotor with period $T_f=f(\theta)+\theta$, drowning out the regular stimuli and subsuming the entire extent of the tissue. The long-term behavior of the tissue is illustrated in Figure 3. This shows three "phase-resetting" plots, which illustrate the phase at a given element as a function of time t (thin diagonal lines) and the APD at that point as a function of t (thick horizontal lines). We show phase-resetting plots for three different elements: the stimulation site (Fig. 3a), an element in the initial 2:1 region (Fig. 3b), and an element in the initial "1:1" (or "transient 2:2") region (Fig. 3c). By t=200 msec, all three points have fallen into the wake of the rotor, and the phase is periodically reset at intervals $T_f= f(\theta)+\theta$. Figure 4 shows a pair of rotors in this simulation at t=235 msec.

Similar results have been found for a small region of 1:1 elements embedded in a 2:1 field (not shown). If the 1:1 elements are transiently alternating about the fixed point, under certain restrictions on σ_1, a stable rotor can be formed. It remains to be determined whether there is an analytical reason which limits the formation of a sustained rotor to cases where the initial conditions are alternating about, rather than settled at, a fixed point. It may be that this limitation is unique to certain choices of parameters in the map (2)-(4), or to certain ranges of σ_1.

Conclusions

We have shown that under some conditions local bistabilities can lead to phase singularities and rotor formation. However, the model presented here is, certainly, only a caricature of cardiac dynamics. First, the map (2)-(4) is itself an imperfect description of cardiac dynamics [8], and a spatial extension of an imperfect local map is bound to give an incomplete picture. Also, the values required of σ_1 may be unrealistically large. The model presented here does not take into account current attenuation as the signal is transmitted further from the stimulus site, nor the dependence of propagation velocity on wave front curvature (e.g., a convex front propagates faster than a concave one). The model does not account for diffusive coupling between elements. The rotation rate of the rotor found here $T_f=f(\theta)+\theta \sim 48$ msec is considerably faster than that observed in experimental preparation [12]. A realistic picture of inhomogeneities such that some regions of tissue would be in a 1:1 state and others in a 2:1 state must also be developed.

Certainly more realistic models must be investigated before a clear hypothesis can be formed about the role of bistability in rotor formation. A next step might be to explore the role of local bistabilities in a spatially extended version of the Luo-Rudy [13] model, for example, using the method of Barkley [14].

Despite these shortcomings, however, this model does reproduce some of the most basic features of propagation in cardiac tissue, and therefore may be considered a "ground-zero" testbed for a study of the spatial effects of bistability. The observation that local bistabilities can lead to phase singularities and rotors in this simple model, along with the observation of bistability in *in vivo* sheep atria at BCL values where complex arrhythmias also occur [9], suggest that local bistability should be seriously investigated, both in more detailed theoretical models of excitable media and in experimental cardiac preparations, as a possible rotor-generating mechanism.

References

1. D. R. Chialvo and J. Jalife, *Nature* **330** (1987) 749.
2. M Guevara, G. Ward, A. Shrier and L. Glass, *Computers in Cardiology*, IEEE Comp. Soc.,(1984) 167.
3. J. B. Nolasco, R. W. Dahlen, *J. Appl. Physiol.* **25** (1968) 191.
4. M. Guevara, A. Shrier and L. Glass, in Zipes DP, Jalife J (eds): Cardiac Electrophysiology, From Cell to Bedside. Philadelphia, PA, WB Saunders Co., 1990, ch. 23.
5. D. R. Chialvo, D. C. Michaels and J. Jalife, *Circ. Res.* **66** (1990) 525.
6. D. R. Chialvo and J. Jalife, in Zipes DP, Jalife J (eds): Cardiac Electrophysiology, From Cell to Bedside. Philadelphia, PA, WB Saunders Co., 1990, ch. 24.
7. G. R. Mines, *J Physiol. (Lond)* **46** (1913) 349.
8. G. M. Hall, S. Bahar and D. J. Gauthier, *Phys. Rev. Lett.* **82** (1999) 2995
9. R. A. Oliver, W. Krassowska, G. M. Hall, S. Bahar, P. D. Wolf and D. J. Gauthier, submitted abstract.
10. P. Berge, Y. Pomeau and C. Vidal, Order Within Chaos: Towards a Deterministic Approach to Turbulence. New York, NY, J. Wiley and Sons, 1984.
11. M. L. Pressler, P. N. Munster and X. Huang, in Zipes DP, Jalife J (eds): Cardiac Electrophysiology, From Cell to Bedside, 2nd ed. Philadelphia, PA, WB Saunders Co., 1995, ch. 16
12. J. M. Davidenko, A. V. Pertsov, R. Salomonsz, W. Baxter and J. Jalife, *Nature* **355** (1992):349.
13. C. H. Luo and Y. Rudy, *Circ. Res.* **68** (1991):1501.
14. D. Barkley. *Physica* **49D** (1991):61.